International Journal of Thermophysics, Vol. 24, No. 6, November 2003 (© 2003)

Dew Point, Liquid Volume, and Dielectric Constant Measurements in a Vapor Mixture of Methane + Propane Using a Microwave Apparatus

E. F. May,[1–3] T. J. Edwards,[1] A. G. Mann,[1] and C. Edwards[1]

Received May 12, 2003

An apparatus based on a microwave resonant cavity has been used to measure dew points and liquid volume fractions in a $zC_3H_8+(1-z)CH_4$ mixture with $z=0.250\pm0.001$ mole fraction. The microwave cavity is optimized for the measurement of small liquid volume fractions in lean natural gases. Argon and carbon dioxide were used to calibrate the resonator for dielectric constant and liquid volume measurements in mixtures. Estimated uncertainties are 1×10^{-4} for dielectric constants and (0.05 K, 0.05 MPa) for dew points. The novel use of multiple cavity modes, each sensitive to different liquid volume regimes, substantially improves the reliability of liquid volume measurements. Liquid volume fractions can be resolved to better than 0.01%. Densities inferred from (P, T, ε) measurements agree within 0.6% of equation of state (EOS) densities with an estimated uncertainty of 0.1%. Liquid volume fractions measured with the microwave apparatus compare well with values determined using a conventional PVT cell. Fourteen dew points were measured at ten different temperatures. From these data, the mixture cricondentherm is estimated to be (293.45 ± 0.05) K, which is 0.15 K higher than the value predicted using the Peng–Robinson equation of state.

KEY WORDS: dew points; dielectric constant; hydrocarbon mixture; liquid volume fraction; microwave cavity; phase behavior.

[1] School of Oil and Gas Engineering and School of Physics, University of Western Australia, Crawley, Western Australia 6009, Australia.

[2] To whom correspondence should be addressed. E-mail: eric.may@nist.gov

[3] Current Address: Process Measurements Division, National Institute of Standards and Technology, Gaithersburg, Maryland 20899, U.S.A.

0195-928X/03/1100-1509/0 © 2003 Plenum Publishing Corporation

1. INTRODUCTION

Lean gas condensate fluids are of increasing significance in petroleum production for both economic and environmental reasons. Optimal extraction and production of these fluids require an accurate knowledge of their phase behavior. In particular, the volume of the valuable condensate phase needs to be determined reliably; however, at most pressures and temperatures of interest the liquid volume fraction is extremely small. The need to tune thermodynamic models to reliable data, together with the inaccuracy of dew points measured by constant bore (three-windowed) PVT cells, led to the development of so-called Sloane PVT cells, specialized for gas condensates. These systems provide reliable phase behavior data by accurately measuring small liquid volumes in large sample sizes. However, Sloane PVT cells are confined to the laboratory, and are often expensive and physically large with corresponding long equilibration times.

The small internal volumes of microwave-based measurement systems result in a considerable reduction in equilibration time. Other advantages include their capacity for automation and the potential for use in the field. Goodwin et al. [1] developed a re-entrant resonator and an analytic model, that was successfully used to determine dew and bubble points in the critical region of an ethane + carbon dioxide mixture. May et al. [2, 3] extended this work by incorporating a similar re-entrant cavity into a variable volume system that could vary sample density without risk of inadvertent changes in composition. May et al. [3] also demonstrated that microwave systems could measure liquid volumes in addition to phase boundaries. However, in that case the re-entrant geometry of the microwave cavity was not optimized for dew-point detection in gas condensate fluids.

May et al. [2, 4] recently reported the development of a new microwave system, designed specifically for phase behavior measurements in lean gas condensates. At the heart of that constant volume system was a microwave cavity with a re-entrant geometry optimized for the detection of dew points and the measurement of small liquid volume fractions. In this paper, the final version of that apparatus—a variable volume microwave PVT cell—is described, together with the results of measurements made on a methane + propane mixture. The same mixture was also studied in a conventional gas condensate PVT cell, and the two sets of experimental data are compared.

EXPERIMENTAL SYSTEM

A schematic of the microwave PVT cell (MPVTC) is shown in Fig. 1. The experimental system is described elsewhere in detail [2, 4, 5] and

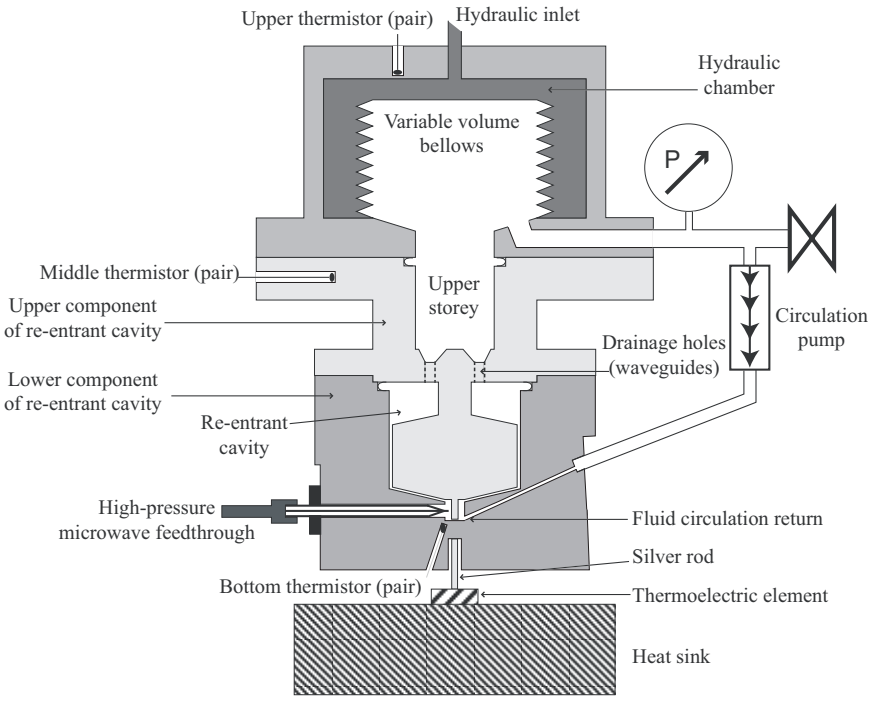

Fig. 1. Schematic of the variable volume microwave PVT cell.

only the essential elements are discussed here. The sample volume of the MPVTC can be separated into four sections, referred to as: the re-entrant cavity, the "upper-story" the variable volume bellows, and the external flow loop. The "upper-story" is electromagnetically isolated from the re-entrant resonator and is redundant in the present system. The variable volume bellows and the re-entrant cavity are connected by the external flow loop, which contains a quartz crystal pressure gauge, the sample inlet valve, and a pneumatically driven, magnetically coupled, circulation pump. The pressure gauge was calibrated *in situ* against a Desgrange et Huot Type 26000M Fundamental Digital Pressure Standard; at pressures below 12 MPa, the estimated pressure uncertainty is ± 0.001 MPa. Sample volume is varied by changing the height of the bellows by means of a hydraulic fluid and a high pressure hydraulic pump. A potentiometer is used to monitor bellows height and, thus, the sample volume.

The re-entrant cavity is shown schematically in Fig. 2. At the top of the re-entrant cavity region, a thin cylindrical neck extends down into an outer cylindrical cavity. The neck then expands into a bulbous coaxial

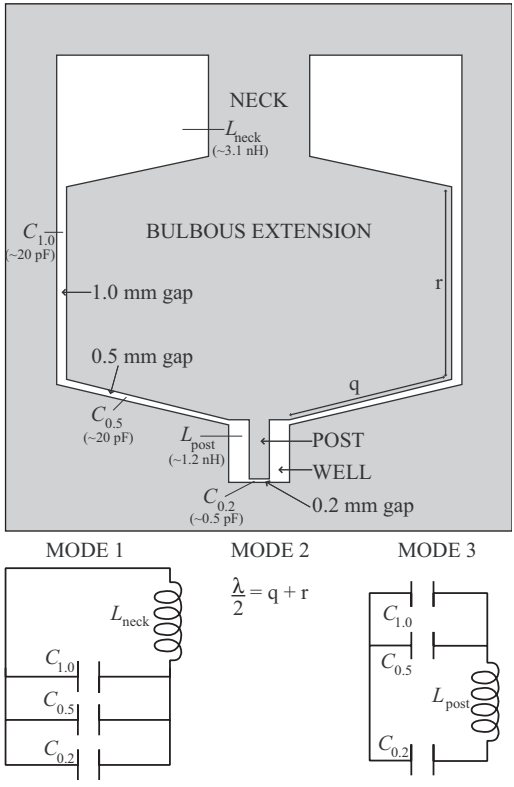

Fig. 2. Schematic of the re-entrant cavity, together with the simplest models for the three measured modes.

extension that nearly fills the hollow interior of the cavity. A 1.0 mm annular gap is formed between the bulbous coaxial extension and the cylindrical wall. The bottom surface of the bulbous extension slopes parallel to the bottom wall of the outer cylinder at a separation of 0.5 mm. The geometry to this point is essentially that employed by Goodwin et al. [1] (although the gap between the bulb bottom and outer cylinder in their resonator was about 5 mm). A 2.0 mm diameter post centered on the bottom of the bulbous coaxial extension extends into a 6.0 mm diameter well, centered in the bottom wall of the outer cylinder. The post terminates 0.2 mm above the bottom of the well.

A novel aspect of this apparatus is that several modes of the re-entrant cavity, each sensitive to different liquid volume regimes, are monitored. This substantially improves the reliability and resolution of liquid volume measurements. To excite all of the desired modes, an electric field probe

enters through the outer wall, 3.0 mm above the bottom of the well. The probe is an extension of the inner conductor of a 40 mm long, high-pressure feedthrough. The first three modes excited by the probe have vacuum frequencies $\approx$ 460 MHz, 4.3 GHz, and 6.9 GHz. Resonant frequencies and half-widths are measured using a vector network analyzer; see Refs. 4 and 5 for further detail.

The properties of the three modes have been modeled with both analytic waveguide descriptions similar to that developed by Goodwin et al. [1], and also with numerical finite element techniques. The simplest models for each of the three modes are shown in Fig. 2. The primary roles of Mode 1 (460 MHz) are the measurement of liquid volumes greater than about 0.7 cm^3, and the determination of single-phase dielectric constants; it is very weakly coupled to the external circuit [6]. Mode 2 (4.3 GHz) is essentially a standing wave confined to the 0.5 and 1.0 mm gaps. Unlike Modes 1 and 3, it is not amenable to description by lumped circuit elements. The principal role of Mode 2 is the measurement of liquid volumes less than 0.7 cm^3. The properties of Mode 3 (6.9 GHz) are determined by the post-well region; this mode has a very intense electric field across the 0.2 mm gap. The role of Mode 3 is dew-point detection as the frequency of this mode is ultra-sensitive to the presence of any liquid phase in this gap.

To realize the system's potential for sensitive dew-point detection, the location at which the liquid phase first forms must be controlled. Three mechanisms are employed to ensure that liquid forms in the cavity's most sensitive region (the 0.2 mm gap between the post and the well). The first of these is drainage. The bottom of the well is the lowest point in the entire system, and where possible, internal surfaces are sloped to facilitate drainage of liquid. The circulation pump provides the second dew focusing mechanism. The low volume external loop terminates in the wall of the well, near the bottom surface. The flow loop allows the 0.2 mm gap to be flushed with fluid from the variable volume bellows. The most important dew focusing mechanism, however, is thermal control. The steady-state temperature distribution of the entire apparatus—including the external circulation loop—is well defined by three, independent, thermal control systems (not completely shown in Fig. 1). One of these systems consists of a thermoelectric element compressed between a heat sink and a cylinder of silver that extends into a recess in the external wall of the re-entrant cavity. The recess and the silver cylinder terminate 5 mm directly below the bottom surface of the well. The well-bottom may thus be cooled by up to 0.5 K relative to the rest of the MPVTC; usually 0.2 K is employed and this ensures that any liquid phase will first form in the cavity's most sensitive region.

The temperature of the MPVTC is monitored by six thermistors and two 100 Ω PRTs. The temperatures reported here are those of the thermistors

monitoring the well-bottom temperature. All eight thermometers were calibrated on three occasions, six months apart, against a capsule type, 25 Ω, standard platinum resistance thermometer (SPRT) which, in turn, had been calibrated to ITS-90. Based on these calibrations, the estimated uncertainty of temperatures reported here is ±0.05 K; this relatively large value is a consequence of long-term thermistor drift caused by thermal cycling.

3. DIELECTRIC CONSTANT CALIBRATION

The work of Hamelin et al. [6] leads to the following equation for the dielectric constant ε of a fluid within a re-entrant resonator [7], in terms of the resonant frequency f, resonant half-width g, and resonant quality factor Q $(= f/(2g)) \gg 1$:

$$\varepsilon = \varepsilon_r + j\varepsilon_i = \left(\frac{f_0 + jg_0}{f + jg}\right)^2 \left(\frac{1 + (-1+j)\, Q^{-1}}{1 + (-1+j)\, Q_0^{-1}}\right) \tag{1}$$

Here, the subscript "0" denotes properties of the vacuum resonance. Hamelin et al. [6] developed this model for ε measurements in high-loss fluids, such as water. For nonpolar fluids, such as hydrocarbon mixtures, ε_i is very small. If it is assumed that all losses are due to the finite conductivity of the boundary metal, then the imaginary terms in Eq. (1) all cancel. For low-loss fluids, the Q factor is essentially determined by the penetration depth δ. Since $\delta^{-1} \propto \sqrt{f}$, to first order in Q^{-1}, Eq. (1) can be simplified;

$$\varepsilon = \left(\frac{f_0}{f}\right)^2 \left[1 + Q_0^{-1}\left(1 - \sqrt{\frac{f_0}{f}}\right)\right] \tag{2}$$

The vacuum resonant frequency f_0 is determined by the (relative) positions of boundary conductors, which vary with resonator temperature T and sample pressure P. For the conditions accessible to the MPVTC, the variation of f_0 is linear with T and P, and thus for each mode n, dielectric constants were determined from the working equation:

$$\varepsilon_{\text{meas},\,n} = \left(\frac{f_{00n}(1 + \theta_{fn}(T - T_0) + \phi_n P)}{f_n}\right)^2 \times \left[1 + Q_{0n}^{-1}\left(1 - \sqrt{\frac{f_{00n}(1 + \theta_{fn}(T - T_0) + \phi_n P)}{f_n}}\right)\right] \tag{3}$$

Here, f_{00n} and Q_{0n}^{-1} are mode n's vacuum resonant frequency and quality factor at $T_0 = 30.00$°C, and θ_{fn} and ϕ_{fn} are the mode's temperature and

Table I. Parameters for Eq. (3) Used to Calculate Mixture Dielectric Constants, with the Estimated Fractional Uncertainties σ_ε for Each Mode

Mode	1	2	3
f_{00} (MHz)	461.305 ± 0.005	4361.90 ± 0.06	6903.9 ± 0.2
$10^6\theta_f$ (K^{-1})	−26.7 ± 0.5	−26.0 ± 0.7	−31 ± 1
$10^4\phi$ (MPa^{-1})	3.50 ± 0.02	1.33 ± 0.02	4.94 ± 0.02
Q_0^{-1}	0.0011 ± 0.0001	0.0017 ± 0.0002	0.0016 ± 0.0002
$10^6\sigma_\varepsilon$	53	68	138

pressure coefficients, respectively. The parameters f_{00n}, θ_{fn}, and Q_{0n}^{-1} can be determined by either direct measurement or by calibrating each mode using helium or argon, fluids with extremely well characterized dielectric properties. The parameters ϕ_n can only be determined by calibration, although they were estimated using coupled electromagnetic-elastic finite element models. The parameter values determined by direct measurement or modeling were consistent with the values determined by calibration. In Table I, the values and uncertainties of f_{00n}, θ_{fn}, ϕ_n, and Q_{0n}^{-1} used in the determination of mixture ε are listed. Estimates of the standard fractional error in the mixture ε for each mode are also shown.

The mode temperature coefficients are all larger than $-20 \times 10^{-6}\ K^{-1}$, the value expected based on literature values of the coefficient of thermal expansion of brass [8]. This is attributed to compression of the pressure seal (a C-ring) between the upper and lower re-entrant cavity components, with increasing temperature. The large uncertainty in f_{00} for Modes 2 and 3 are a result of hysteresis in the resonator dimensions—particularly the 0.2 mm gap—with pressure cycling; this is also associated with the C-ring seal. However, Mode 1 is insensitive to this hysteresis and it is also very weakly coupled to the external circuit. Mixture dielectric constants reported here are those determined with Mode 1, and have an estimated uncertainty of less than 1×10^{-4} (coverage factor of 2).

4. LIQUID VOLUME CALIBRATION

At two-phase conditions, all three $\varepsilon_{\text{meas},n}$ values are used to provide three independent estimates of the liquid volume in the cavity. The $\varepsilon_{\text{meas},n}$ values are effectively all the same for a single-phase fluid but, when the re-entrant cavity contains a two-phase fluid, the $\varepsilon_{\text{meas},n}$ are different since they depend upon the vapor- and liquid-phase dielectric constants ε_{vap} and ε_{liq}, the electric field distribution of the mode, and the location and amount

of liquid in the cavity. A mode may be characterized by a normalized quantity G_n which we call the mode shape function, defined by

$$G_n = \frac{\varepsilon_{\text{meas},n} - \varepsilon_{\text{vap}}}{\varepsilon_{\text{liq}} - \varepsilon_{\text{vap}}} \tag{4}$$

The usefulness of G_n depends entirely upon (a) the continuity of the liquid phase within the cavity and (b) the reproducibility of the way in which liquid fills and drains from the cavity; these constraints will henceforth be implicitly incorporated into the definition. The mode shape function reflects the distribution of electric fields for a given mode throughout the cavity, and how two fluid phases interact with that distribution. For non-polar materials, it may be expected that this field distribution be nearly fluid independent, and thus it is useful in extracting liquid volume information from that mode's frequency response. The relation between the mode shape function and the liquid volume within the cavity V_L, is single-valued and monotonic. Initial measurements with *n*-decane and carbon dioxide indicate that, to a reasonable approximation, the functions $G_n(V_L)$ are, in fact, fluid independent [5]. Thus, by measuring the $G_n(V_L)$ with a reference fluid, the frequency responses of each mode can be calibrated for subsequent liquid-volume determinations in two-phase mixtures.

The MPVTC was calibrated with CO_2 (99.99% minimum molar purity) at 17.73°C by filling the cell at maximum volume to a pressure of 4.887 MPa. Sample volume was changed in decrements of between about 1 and 5 cm^3 until the minimum system volume was reached. The frequency of Mode 3, f_3, was used to identify the dew-point pressure P_{dew}. The measured value agreed with the saturation pressure for this isotherm calculated using the reference equation of state (EOS) of Span and Wagner [9], within the temperature uncertainty of the MPVTC. This EOS was used to calculate the bulk fluid density, vapor mole fraction, and liquid volume corresponding to each steady-state condition. At minimum system volume the amount of liquid present was in excess of 25.8 cm^3, which is larger than the estimated volume required to completely fill the re-entrant cavity (21 cm^3). The sample was then expanded back to its initial condition, in volume increments similar in magnitude to those used during the compression.

The value of ε_{vap} used in Eq. (4) was taken to be that of $\varepsilon_{\text{meas},1}$ ($= 1.0938$) at the last single-phase point. For all liquid volumes larger than 21.4 cm^3, the values of $\varepsilon_{\text{meas},n}$ were 1.4830, 1.4869, and 1.4725, for Modes 1, 2, and 3, respectively. The saturated liquid CO_2 measurements of Haynes [10] lead to an estimate for $\varepsilon_{\text{liq}} = 1.4796 \pm 0.0007$ at this temperature. In terms of $(\varepsilon - 1)$, this is only 0.7% smaller than the maximum value of $\varepsilon_{\text{meas},1}$. The discrepancy between the three modes illustrates systematic

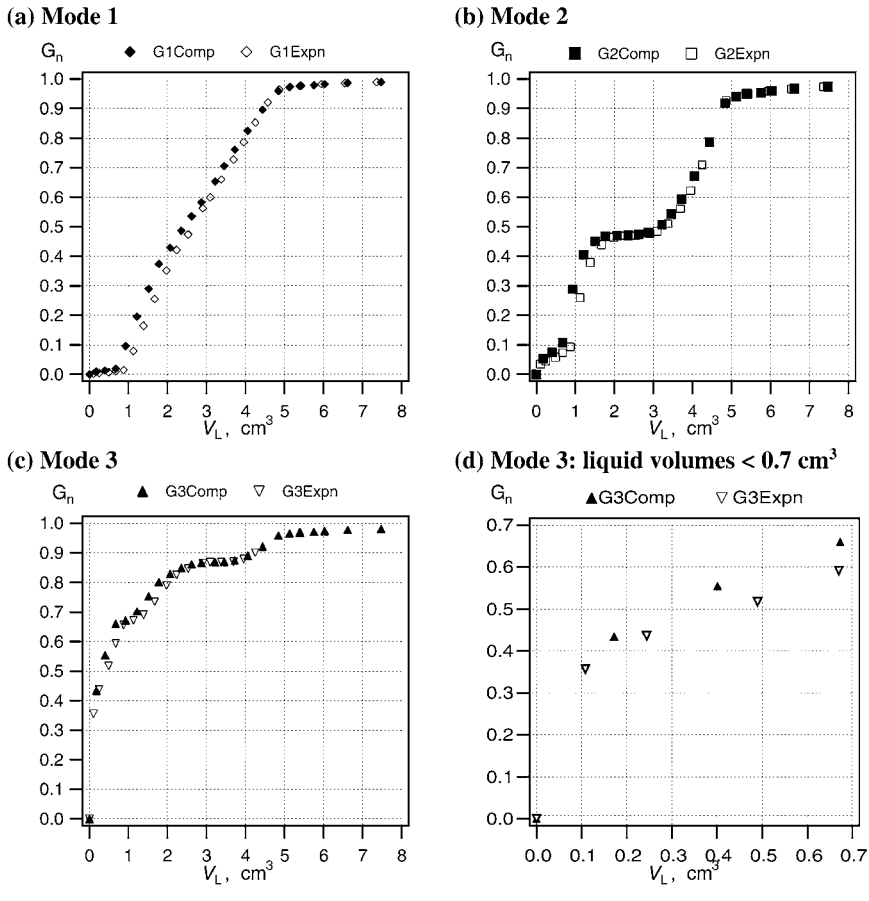

Fig. 3. Mode shape functions as a function of liquid volume, determined from an isothermal calibration with carbon dioxide.

errors associated with large ε measurements using Modes 2 and 3; the cause of this is under investigation. To maintain the G_n normalization requirement, the value of ε_{liq} used in Eq. (4) was taken to be the maximum value of ε_{meas} determined by each mode. The mode shape functions derived from this CO_2 calibration are shown as a function of liquid volume in Fig. 3.

Only data for $V_L \leqslant 8\ cm^3$ are shown in Fig. 3 as the variation in G_n for larger liquid volumes is less than 3% for all modes. There is a small amount of hysteresis apparent, most noticeable in G_1 and G_2 for $0.5\ cm^3 \leqslant V_L \leqslant 2\ cm^3$. This hysteresis is due to the differences that exist between the condensation/filling process and the evaporation/draining process. It is likely that surface effects make the latter less reproducible

than the former. Furthermore, experimental control of expansions is not as refined as the control of compressions, which may contribute to the reduced repeatability of liquid evaporation.

Comparison of two-phase mixture $\varepsilon_{\text{meas},n}(P)$ curves with these carbon dioxide $G_n(V_L)$ curves allows mixture liquid volumes to be deduced [5]. The characteristics of the $G_n(V_L)$ curves indicate the differing sensitivities of each mode to different liquid-volume regimes. The linearity of $G_1(V_L)$ between about 0.7 and 5.0 cm^3 makes it the most useful mode for all but small liquid volumes. The extremely steep initial slope of $G_3(V_L)$ makes it an optimal dew-point detector, but it also becomes "saturated" at small liquid volumes. Mode 2 has good sensitivity up to about 1.3 cm^3; it is the most accurate mode for $V_L < 0.7$ cm^3, and the redundancy with Mode 1 for larger volumes improves the overall reliability of liquid-volume determinations.

5. MIXTURE MEASUREMENTS

A $zC_3H_8 + (1-z)CH_4$ mixture, with $z = 0.250 \pm 0.001$ mole fraction, was prepared gravimetrically in a high-pressure, 500 cm^3 sample cylinder, using a 10 kg capacity balance with an uncertainty of ± 3 mg. Mixing was achieved by shaking, a metal ball having been placed inside the cylinder. The mixture mole fraction uncertainty is due primarily to impurities (predominantly isobutane) in the propane, which had a stated minimum purity of 99.58% by mole. The methane used had a stated minimum purity of 99.99% by mole. A cricondentherm of 20.15°C was predicted for this mixture using the Peng–Robinson (PR) EOS [11].

5.1. Single-Phase Density Determinations

Mixture dielectric constants at various pressures were measured along four isotherms between 23 and 32°C; the data are listed in Table II. At each condition an inferred density ρ_{inf} is listed based on the measured ε, the propane mole fraction z, and Eq. (5).

$$\rho_{\text{inf}} = \left(\frac{\varepsilon - 1}{\varepsilon + 2}\right)(zP_{tC3} + (1-z)\,P_{tC1})^{-1} \tag{5}$$

Here, P_{tC3} and P_{tC1} are the total molar polarizabilities of propane and methane, respectively, estimated from the correlations of Schmidt and Moldover [12], which are functions of density. The EOS of Setzmann and Wagner [13] was used to calculate the methane density corresponding to the mixture temperature and pressure. For propane, however, the saturated vapor density corresponding to the mixture temperature was used,

Table II. Temperatures (°C), Pressures (MPa), and Dielectric Constants for the Binary Mixture, with Densities ($mol \cdot dm^{-3}$) Calculated from Component Polarizabilities. Deviations (%) of These Densities from Lemmon's EOS [15] are also Listed. ($Dev = 100(\rho_{inf} - \rho_{EOS})/\rho_{EOS}$)

T	P	ε	ρ_{inf}	Dev	T	P	ε	ρ_{inf}	Dev
31.79	5.928	1.0836	3.04	0.5	28.81	5.847	1.0840	3.05	0.5
31.77	7.065	1.1066	3.84	0.6	25.87	5.715	1.0834	3.03	0.5
31.76	8.109	1.1299	4.65	0.5	25.89	6.586	1.1018	3.68	0.6
31.76	9.063	1.1526	5.42	0.4	25.89	7.499	1.1231	4.42	0.6
31.76	9.994	1.1755	6.19	0.3	22.93	5.496	1.0809	2.94	0.5
31.77	5.961	1.0842	3.06	0.5	22.93	6.733	1.1082	3.90	0.6
28.83	5.859	1.0842	3.06	0.5	22.93	7.634	1.1308	4.68	0.6
28.82	7.000	1.1080	3.89	0.6	22.93	8.516	1.1546	5.49	0.5
28.82	8.853	1.1525	5.42	0.4	22.94	9.349	1.1782	6.28	0.3
28.82	9.732	1.1750	6.17	0.2	22.94	5.581	1.0827	3.01	0.6

calculated with the EOS of Miyamoto and Watanabe [14]. The inferred densities are compared with those calculated using Lemmon's EOS [15], which has an estimated uncertainty of $\pm 0.1\%$.

May et al. [16] compared measured molar polarizabilities in mixtures of $CH_4 + C_3H_8$ and $CH_4 + C_3H_8 + C_6H_{14}$ with those calculated from literature correlations. However, they used both the measured mixture temperature *and* pressure to calculate the propane density used in the polarizability correlation. This leads to a (larger) value for P_{tC3}, characteristic of propane at liquid densities, as opposed to a (smaller) value more representative of the actual number of propane molecules per unit volume present in the mixture. If their data are re-analyzed using saturated propane vapor densities based on the mixture temperatures, the agreement between their measured and predicted mixture polarizabilities improves from 0.5 to 0.2%, which is within the uncertainty of their experimental values.

Although the ρ_{inf} here are systematically larger than the EOS densities, the deviations are small, with an average of 0.5%. These results are significant because they demonstrate that MPVTCs could be used to measure single-phase mixture densities with an uncertainty comparable to that of vibrating tube densimeters, which are known to suffer from systematic errors associated with gas sonic speed [17, 18]. In custody transfer situations, for example, conventional densimeter-chromatograph systems could be replaced with MPVTC-chromatograph systems, with the advantage that the process stream's dew point could be measured directly rather than calculated from an EOS.

5.2. Two-Phase Measurements

Fourteen dew points were measured isothermally at ten different temperatures. The pressures and temperatures of the measured dew points are shown in Fig. 4 and listed in Table III, together with dew points predicted using the PR EOS. Liquid volume fractions were measured isothermally at 18.90 and 16.90°C; the P and T of these measurements are also shown in Fig. 4. An estimate of the cricondentherm based on the six dew points measured at 19.90, 20.10, and 20.20°C was made by regressing them to a quadratic function of pressure. The estimated mixture cricondentherm temperature is (20.30 ± 0.05)°C, which is 0.15°C higher than the value predicted using the PR EOS.

The basis of the dew-point uncertainty estimates is illustrated by the results of a constant mass expansion conducted at 16.90°C, commencing at a sample pressure of 8.672 MPa. Measured values of f_3 in the vicinity of the upper dew point are shown in Fig. 5 for both the expansion into the two-phase region, and the subsequent compression out of it. For all the measurements discussed in this section, the sample was mixed for six minutes twice per data point, usually immediately after the pressure change

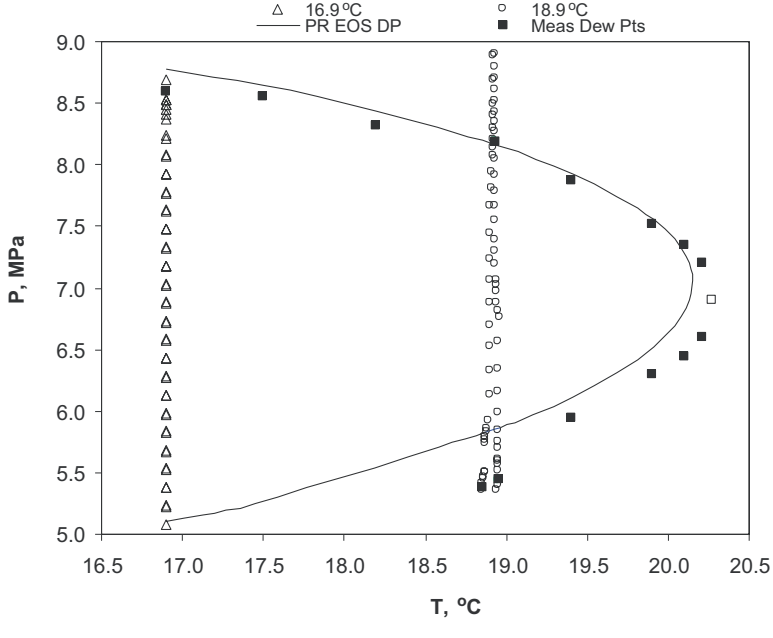

Fig. 4. Summary of the two-phase measurements in the (P, T) plane. The hollow square is the estimated cricondentherm. PR EOS predictions are also shown.

Table III. Measured and Peng–Robinson (PR) EOS Dew Points for the Binary Mixture

Measurement (±0.05°C, ±0.05 MPa)		PR EOS
T (°C)	P (MPa)	P (MPa)
16.90	8.60	8.78
17.50	8.55	8.65
18.20	8.32	8.43
18.93	8.19	8.16
19.41	7.87	7.93
19.91	7.52	7.56
20.11	7.35	7.26
20.21	7.20	Single-phase
20.21	6.60	Single-phase
20.11	6.44	6.84
19.91	6.30	6.52
19.41	5.95	6.12
18.96	5.44	5.87
18.85	5.38	5.82

and again 0.5 hours later. A minimum of two hours per data point was allowed for equilibration.

The three highest pressure expansion data points are all at very similar values of f_3. The slight frequency increase as the pressure is decreased is characteristic of a single-phase fluid. In contrast, the pressure decrease

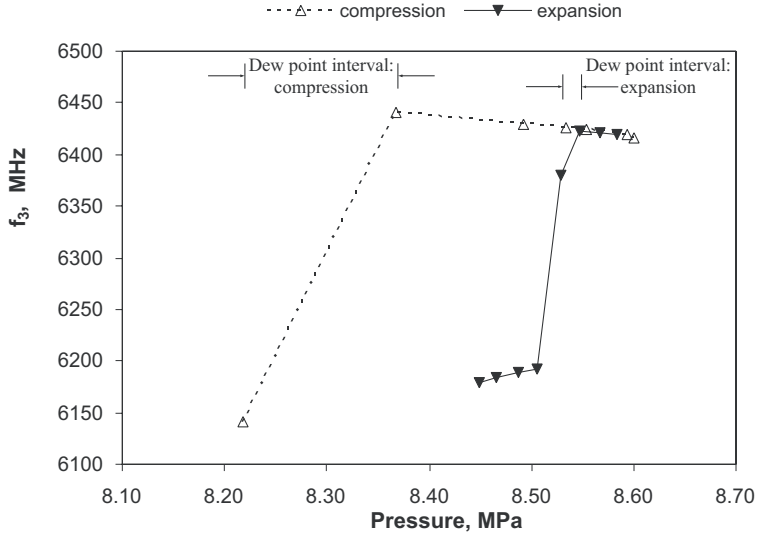

Fig. 5. Mode 3 frequency at 16.90°C near the binary mixture's upper dew point.

from 8.547 to 8.530 MPa results in a frequency *decrease* of more than 40 MHz. The upper dew point pressure P_{UD} measured in expansion is, therefore, (8.54 ± 0.01) MPa. However, the compression data series gives $P_{UD} = (8.29 \pm 0.08)$ MPa. This is an example of the hysteresis that was observed in several dew-point determinations at temperatures below 18.90°C. It was found that for measurement pathways starting in the two-phase region and going into the single-phase region, the apparent dew point occurs at an earlier pressure than for pathways commencing at a single-phase condition and entering into the two-phase region. The current MPVTC is optimized to detect the onset of dew in single-phase "gas," and thus dew points determined along pathways commencing within the two-phase region are likely subject to more significant systematic effects. Thus, the dew points listed in Table III are based only on dew points detected by the expansion or compression of single-phase fluids.

The rate of measurement was also found to affect the value of P_{UD} determined along measurement pathways commencing in the single-phase region. It was found that if less than two hours per pressure step were allowed, the faster the expansion rate, the lower the measured value of P_{UD}. For this reason, the dew points listed in Table III are an average of all determinations made at that temperature commencing in the single-phase region, with at least two hours per pressure step. An uncertainty of ± 0.05 MPa is estimated to account for the impact of any other systematic effects.

Liquid volume fractions (LVF), measured in compression and expansion with the MPVTC at 16.90°C, are shown in Fig. 6. Also shown are values predicted using the PR EOS, an estimate of the maximum liquid volume fraction based on the data of Reamer et al. [19] and LVF for the same mixture, measured using a Sloane PVT cell in our laboratory.

The differences between the three experimental data sets are significantly smaller than the disparity of those sets with the EOS values. The P_{UD} value predicted using the PR EOS is 8.78 MPa, which is more than 0.18 MPa higher than the value of P_{UD} determined using the MPVTC and the Sloane PVT cell. These two measurements ((8.60 ± 0.05) MPa for the MPVTC determination and (8.65 ± 0.05) MPa for the Sloane determination) are in good agreement. The lower dew point pressure P_{LD} predicted using the PR EOS is 5.10 MPa; at this condition an LVF of 0.03% was measured using the MPVTC. The pressure predicted for the maximum liquid volume fraction is 7.2 MPa, which is in excellent agreement with the MPVTC value of (7.18 ± 0.07) MPa. Of course, it is well known that LVF predictions from cubic EOS are invariably overestimated [20] and a volume translation correction [21] would normally be applied to force closer agreement between the predicted and measured values.

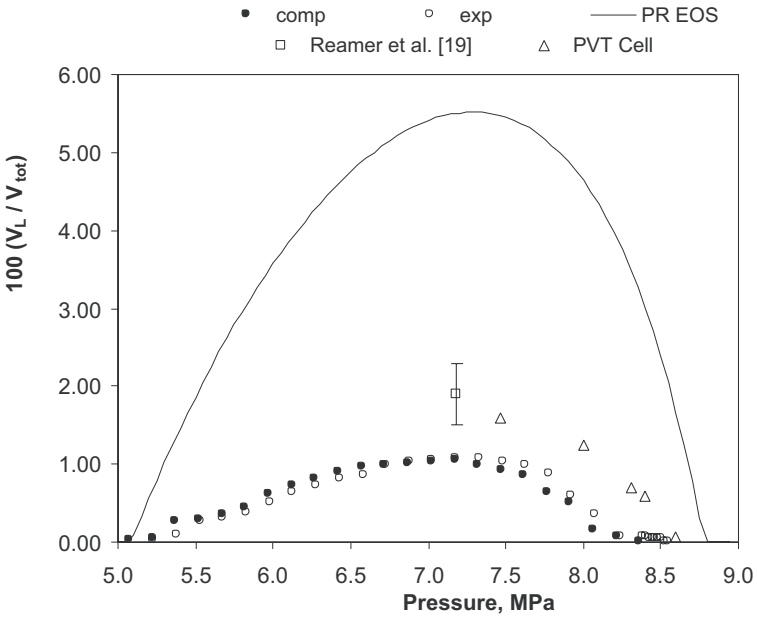

Fig. 6. Liquid volume fractions for the binary mixture at 16.90°C.

A flash calculation using the equilibrium ratios for methane and propane measured by Reamer et al. [19] was used to estimate a liquid volume fraction of $(1.9 \pm 0.4)\%$ at 7.173 MPa. The uncertainty of this estimate is based solely on the stated precision of their composition measurements. This estimate is more consistent with the Sloane PVT cell data (LVF = 1.58% at 7.47 MPa) than with the maximum LVF of 1.07% measured with the MPVTC. The Sloane PVT cell determined a $P_{UD} = (8.65 \pm 0.05)$ MPa from expansion data and a $P_{UD} = (8.85 \pm 0.05)$ MPa from compression data. The 0.2 MPa difference between the Sloane PVT cell dew-point determinations indicates that hysteresis in the measurement of dew points is a feature common to both the MPVTC and conventional instruments.

6. CONCLUSIONS

The phrase "proof of concept" summarizes the principal achievement of this work. The MPVTC can determine hydrocarbon dew points in gas condensate-like systems with very high resolution. In addition, liquid-volume-fraction information can be extracted from microwave measurements made at two-phase conditions. The novel use of multiple cavity

modes, sensitive to different liquid-volume regimes, dramatically improves the resolution and reliability of liquid-volume measurements. Furthermore, with the ability to determine single-phase densities and hydrocarbon dew points, there is significant potential for the use of MPVTCs in custody transfer of natural gas.

While these achievements are substantial, the current system suffers from some limitations. The current cell is not optimized for chemical equilibrium because the design process focused on dew-point sensitivity. The mixing that results from operation of the circulation pump is violent; any liquid present in the cell bottom is "blasted" up into the cell. This exacerbates another limitation of the current cell: excessive liquid hold-up and inadequate drainage are deficiencies that probably result in systematic underestimates of liquid volumes. However, the MPVTC binary mixture data, which provide a reasonable picture of the fluid's phase behavior at this temperature, were measured automatically in less than 96 hours. To obtain a similar set of LVF measurements with the Sloane PVT cell would require between 10 and 100 times longer (based on the duration of the PVT cell experiment described above).

ACKNOWLEDGMENTS

The authors would like to thank the Minerals and Energy Research Institute of Western Australia, Woodside Energy Ltd., and Vision Reservoir Management Technologies International for their support. One of us (EFM) acknowledges the support of a Gledden scholarship from the University of Western Australia. We also thank John Moore, John Budge, and Chris Ballam of the Physics and Engineering Workshops for construction of the apparatus. The authors are indebted to Reid Miller for all of his significant contributions to this project, and are also grateful to Michael Moldover for carefully reading the manuscript.

REFERENCES

1. A. R. H. Goodwin, J. B. Mehl, and M. R. Moldover, *Rev. Sci. Instrum.* **67**:4294 (1996).
2. E. F. May, T. J. Edwards, A. G. Mann, and C. Edwards, International Patent (Australia) PCT/AU01/00784 (2001).
3. E. F. May, T. J. Edwards, A. G. Mann, C. Edwards, and R. C. Miller, *Fluid Phase Equilib.* **185**:339 (2001).
4. E. F. May, T. J. Edwards, A. G. Mann, and C. Edwards, paper presented at the European Conference on Thermophysical Properties, Imperial College, London, United Kingdom, September 1–4, 2002, submitted to *Fluid Phase Equilib.*
5. E. F. May, Ph.D. thesis, University of Western Australia, Perth, Australia (2003).
6. J. Hamelin, J. B. Mehl, and M. R. Moldover, *Rev. Sci. Instrum.* **69**:255 (1998).

7. G. S. Anderson, R. C. Miller, and A. R. H. Goodwin, *J. Chem. Eng. Data* **45**:549 (2000).
8. M. Bauccio, ed., *ASM Metals Reference Book* (ASM International, Meterials Park, Ohio, 1993).
9. R. Span and W. Wagner, *J. Phys. Chem. Ref. Data* **25:**1509 (1996).
10. W. M. Haynes, *Adv. Cryo. Eng.* **31:**1199 (1986).
11. D. Peng and D. B. Robinson, *Ind. Eng. Chem. Fundam.* **15**:59 (1976).
12. J. W. Schmidt and M. R. Moldover, *Int. J. Thermophys.* **24**:375 (2003).
13. U. Setzmann and W. Wagner, *J. Phys. Chem. Ref. Data* **20:**1061 (1991).
14. H. Miyamoto and K. Watanabe, *Int. J. Thermophys.* **21**:1045 (2000).
15. E. W. Lemmon, Ph.D. thesis, University of Idaho, Moscow, Idaho (1996).
16. E. F. May, R. C. Miller, and A. R. H. Goodwin, *J. Chem. Eng. Data* **47**:102 (2002).
17. D. Fawcett, Ph.D. thesis, Murdoch University, Perth, Australia (1995).
18. T. J. Edwards, D. J. Pack, R. D. Trengove, and D. Fawcett, *Proc. International Gas Union, 19th World Gas Conference*, Milan, Italy (1994), pp. 211–226.
19. H. H. Reamer, B. H. Sage, and W. N. Lacey, *Ind. Eng. Chem.* **42**:534 (1950).
20. A. Danesh, *PVT and Phase Behaviour of Petroleum Reservoir Fluids* (Elsevier, Amsterdam, The Netherlands, 1998).
21. A. Peneloux, E. Rauzy, and R. Freeze, *Fluid Phase Equilib.* **8**:7 (1982).